



# Probing into the pristine basic morphology of high impact polypropylene particles

Yong Zhou<sup>a,b</sup>, Hui Niu<sup>a</sup>, Lei Kong<sup>a,b</sup>, Ying Zhao<sup>a</sup>, Jin-Yong Dong<sup>a,\*</sup>, Dujin Wang<sup>a,\*</sup>

<sup>a</sup> Beijing National Laboratory for Molecular Sciences, CAS Key Laboratory of Engineering Plastics, Institute of Chemistry, Chinese Academy of Sciences, Beijing 100190, China

<sup>b</sup> Graduate School of Chinese Academy of Sciences, Beijing 100049, China

## ARTICLE INFO

### Article history:

Received 7 May 2009

Received in revised form

19 July 2009

Accepted 26 July 2009

Available online 29 July 2009

### Keywords:

High impact polypropylene

Morphological observation

Pristine basic structure

## ABSTRACT

In this paper, the pristine basic morphology of high impact polypropylene (hiPP) particles prepared with an industrial  $\text{MgCl}_2/\text{TiCl}_4$  Ziegler–Natta catalyst undergoing sequentially occurred propylene (P) homopolymerization and ethylene (E)/propylene copolymerization has been probed mainly using transmission electron microscopy (TEM) techniques including plain TEM and the advanced transmission electron microtomography (TEMT). It is revealed that the basic structure units comprising a whole hiPP particle are the submicron PP (polypropylene) globule and nano-sized EP (ethylene-co-propylene) droplet. EP rubber (EPR) domain is formed by the agglomeration of EP droplets. Continually formed EP droplets turn to fill, from inside out, the micro- and macro-pores inside the preformed PP skeleton, affording different-sized EPR domains. Taking the two basic structure units into account, new quaternary structure model describing the manifold structures of hiPP particles has been proposed. From these findings, it is suggested that, to gain hiPP polymers with excellent stiffness/toughness-balanced properties, it is crucial to control the first-staged propylene homopolymerization alongside a rational design of the catalyst architecture to accomplish desired EPR dispersion morphologies that dictate hiPP properties.

© 2009 Elsevier Ltd. All rights reserved.

## 1. Introduction

High impact polypropylene (hiPP) is an important type of polyolefin resin synthesized following the “Reactor Granule Technology” (RGT) principle with a 4th or 5th generation spherical Ziegler–Natta (mostly spherical  $\text{MgCl}_2/\text{TiCl}_4$ /electron donor) providing a porous reaction bed for the polymerization of various olefinic monomers [1]. With such a Ziegler–Natta catalyst, two sequentially occurred polymerizations, first propylene homopolymerization then ethylene/propylene random copolymerization, render an in situ blend of plastic polypropylene (PP) and elastomeric ethylene–propylene copolymer (EPR), with the products mimicking the shape of the catalyst but with enlarged bulk [2]. Materials made of hiPP are generally featured by excellent balances of flexural modulus and impact strength, which are usually attributed to the desired phase morphology where the elastomeric EP is dispersed in PP matrix at some submicron level (few hundred nanometers) [3]. For now, hiPP has been listed as one of the fastest growing polymers among the whole family of commercialized polymeric materials. Properties of hiPP mainly depend on its morphology, i.e., dispersion fineness and homogeneity of EPR in PP

matrix, which are evolved during the two successive stages of polymerizations on the granular catalyst reactor (Fig. 1) [4].

Tremendous commercial success has been achieved with hiPP, however, as far as the very important hiPP morphology is concerned, its evolution has not been unambiguously understood, especially when it comes to how EPR phase is formed within a preformed PP skeleton [5]. To understand the formation of the phase morphology of hiPP, many investigations have been carried out in the last two decades to explore the nascent structure of the hiPP granules [5–10]. On this aspect, the nascent hiPP granule is usually described by the replication of the original catalyst morphology, i.e., the shape of polymer particles is controlled by the morphology of catalysts [5,8,10–12]. Kakugo reported that the hiPP particles may have tertiary structures: primary particle (0.2–0.35  $\mu\text{m}$  in diameter), subparticle (ca. 1  $\mu\text{m}$  in diameter), and ultimate particle with diameter ranging from several hundred microns to several millimeters [10]. Du argued that the granule growing of nascent polypropylene/ethylene–octene copolymer hiPP follows the “fractal (self-similar) growth and pore-filling” mechanism [7]. According to this mechanism, the multiple structure of polyolefin alloys ranges from several nanometers to micrometers. Several other mechanisms for the polymerization process of polyolefin alloys have also been proposed, such as “solid core model”, “polymer flow model”, “multi-grain model”, “pore-filling model”, and so on [7,13–15]. In order to interpret the dispersion of EPR in the

\* Corresponding authors. Fax: +86 10 82612857.

E-mail addresses: [jydong@iccas.ac.cn](mailto:jydong@iccas.ac.cn) (J.-Y. Dong), [djwang@iccas.ac.cn](mailto:djwang@iccas.ac.cn) (D. Wang).

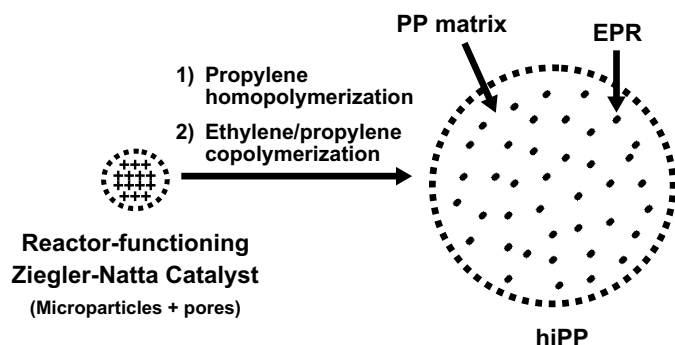


Fig. 1. Formation of hiPP from a reactor-functioning  $\text{MgCl}_2/\text{TiCl}_4$  catalyst.

preformed iPP porous particles, most researches support the “pore-filling model” [6,7,16,17]. According to this model, EPR phase tends to surround the iPP particles and fill the pores, thus smoothing the surface of iPP particles.

Although much progress has been made on the morphology characterization and granule growth mechanism of hiPP, the details of the multiphase structure in hiPP and rubber phases still remain ambiguous, the clarification of which not only aids in understanding the structure–property relationship of hiPP, also feeds back for catalyst design. In this contribution, resorting to state-of-the-art transmission electron microscopy (TEM) techniques, we thrust into the very basic structural level of nascent hiPP particles and, for the first time, reveal that the basic structure units comprising a whole hiPP particle are the submicron PP crystallites and crevice-filling nano-sized EP droplets. EPR phase is formed by EP droplets agglomeration. In light of the generally accepted knowledge that there exist different levels of pores inside a preformed PP architecture [7–10], continually formed EP droplets turn to fill, from inside out, these pores forming different-sized EPR domains. The results of electron microscopy observations indicate that there exists an interesting quaternary structure in a synthesized hiPP nascent particle, and a possible model has been proposed to illustrate the process of the granule growth.

## 2. Experimental section

### 2.1. Materials

The nascent high impact polypropylene (hiPP) particles were prepared by a sequential, two-stage polymerization process

exercised as propylene homopolymerization followed by ethylene/propylene copolymerization catalyzed by the state-of-the-art  $\text{MgCl}_2/\text{TiCl}_4$  supported catalyst bearing 9.9-bis(methoxymethyl)-fluorine (BMMF) internal electron donor. The weight average molecular mass was determined to be  $4.7 \times 10^5$ , with a polydispersity index of 6.5 (GPC). The average content of EPR in the hiPP particles was determined to be 18 wt% by solvent extraction with boiling *n*-heptane.

### 2.2. Field-emission scanning electron microscopy (SEM) measurement

The particle size and surface morphology of the sample were examined with a JEOL JSM-6700F field emission scanning electron microscope at an accelerating voltage of 5 kV. In order to clearly see the PP primary particles, the cross-section of the hiPP nascent particles were etched with xylene at 30 °C for 8 h.

### 2.3. Transmission electron microscopy (TEM) and transmission electron microtomography (TEMT) measurements

For TEM observations, the hiPP particles were first immersed in 1,7-octadiene for 3 h at room temperature, then exposed in atmosphere for 2 min, followed by staining over 1% aqueous solution of  $\text{OsO}_4$  at 60 °C for 3 h, and finally imbedded in EPON™ 812 resin and sectioned with glass knife operated at –110 °C [11]. The microtomed thin sections were transferred onto copper grids and further stained with  $\text{RuO}_4$  for 0.5 h at room temperature. The thin sections were 80–150 nm in thickness. Bright field (BF) electron micrographs were obtained with a JEOL JEM-2200FS transmission electron microscope operated at 200 kV.

In TEMT experiments, a series of TEM projections were recorded with JEOL JEM-2200FS at 200 kV using a single-axis tilt stage. Images were recorded at 8000× magnification at 1° increments of tilt angle, beginning at –70° and finishing at +70°, for a total of 141 images. A cooled CCD camera with 1024 × 1024 pixel elements (Gatan 794, Gatan Inc.) was used to digitally acquire the projected images. The pixel resolution of the projection was 2.03 nm, and the exposure time for each projection was 4s. The tilted series were then aligned by Composer, a commercial software package provided by JEOL, and then reconstructed based on the filtered back projection method [18]. The series of reconstructed images, all aligned with respect to the tilt axis (here, the *y*-axis), was summed to form the 3D volume data.

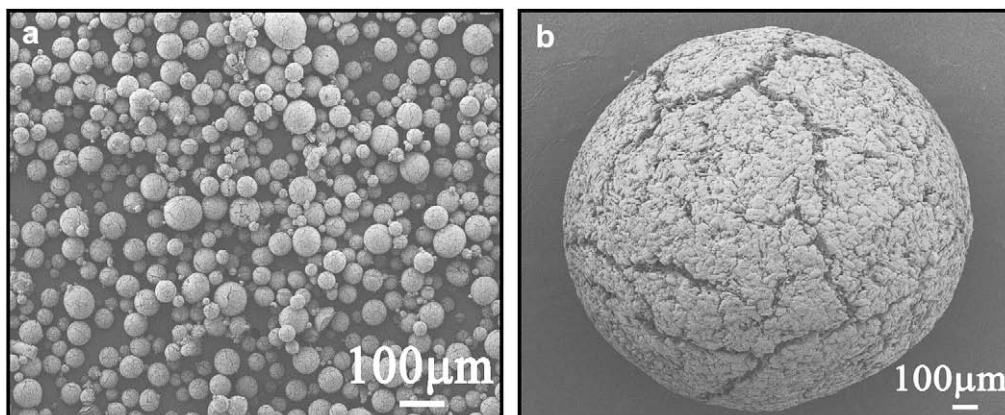


Fig. 2. SEM photographs of (a) the catalyst particles and (b) the selected hiPP particle derived therefrom.

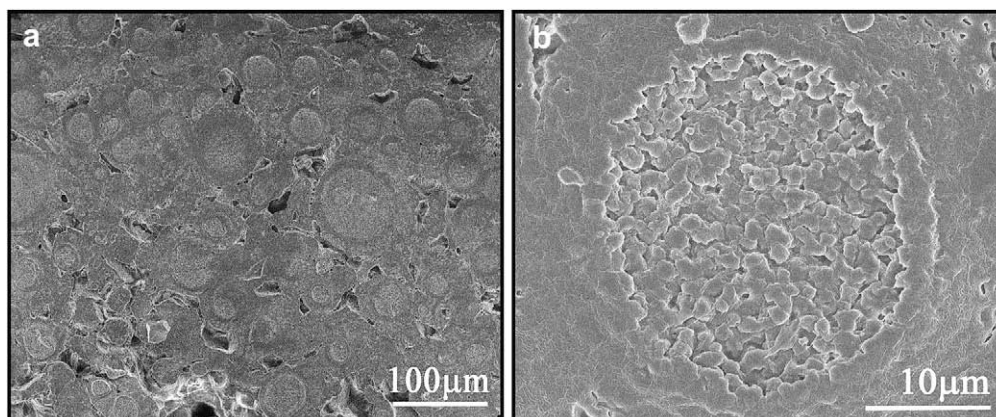


Fig. 3. SEM micrographs of the internal morphology of a nascent hiPP particle: (a) etched at 30 °C with xylene, (b) higher magnification.

### 3. Results and discussion

hiPP particles were prepared using a spherical  $\text{MgCl}_2/\text{TiCl}_4$  catalyst bearing 9,9-bis(methoxymethyl)fluorine (BMMF) as an internal electron donor, with  $\text{AlEt}_3$  as the cocatalyst. The picture of the catalyst particles is shown in Fig. 2(a), from which one can see that, although spherical in general, the catalyst particles are not very homogeneous in size (in the range of 30–80  $\mu\text{m}$ ). Correspondingly, the sizes of the hiPP particles are discrepant in between 600 and 2000  $\mu\text{m}$ . The average content of EPR in these particles is determined to be 18 wt% by solvent extraction using boiling *n*-heptane. One particle with a diameter of 1500  $\mu\text{m}$  was randomly picked up from the mass of the hiPP particles as a representative (Fig. 2(b)). In a nearly perfect spherical shape, it is obvious that the architecture of the hiPP particle (PP skeleton) must have been generated through a strictly implemented catalyst/polymer morphology replication where polymer expansion is accompanied by macro- and micro-pores formation as well as catalyst fragmentation.

Fig. 3 shows the micrograph of the partial cross-section of a hiPP particle after cryo-microtomed and etched with xylene at 30 °C. The nascent hiPP particle ( $d = 1500 \mu\text{m}$ ) is composed of subglobules ( $d = 20\text{--}100 \mu\text{m}$ ) (Fig. 3a), which are agglomerated with much smaller-sized particles ( $d = 1\text{--}3 \mu\text{m}$ ) (Fig. 3b). From the SEM

micrograph, it can be concluded that the nascent hiPP particles temporarily show a tertiary structure.

According to the densely stacking principle of sphere particles, the architecture of nascent hiPP particles is expressed by the following equation:

$$R \approx 0.74 \times \left( \frac{r_1}{r_2} \right)^3$$

where  $R$  is the content of subparticles (the radius is  $r_2$ ) in higher-up particles (the radius is  $r_1$ ), and 0.74 is the constant of hypothesized hexagonal stack of spherical particles. The above equation is not a restrict description of the particle stacking; however, this simplification does not affect the essential features of the analysis. It is estimated that thousands of smaller particles compose of one subglobule, and thousands of subglobules form one nascent hiPP particle. However, SEM technique could not detect the primary PP crystallites, which are believed to have a diameter of several hundred nanometers.

The hiPP particle was then subjected to TEM study to explore its microstructure. To warrant a high authenticity of the TEM observation, a series of specially designed sample treatment procedures in which 1,7-octadiene is used to strengthen the oxidative staining effect on EPR, were adopted to prepare the specimens [11,19]. Fig. 4 shows the typical TEM images of a microtomed thin section of the hiPP particle after stained with  $\text{OsO}_4$  for 3 h. Segregated white,

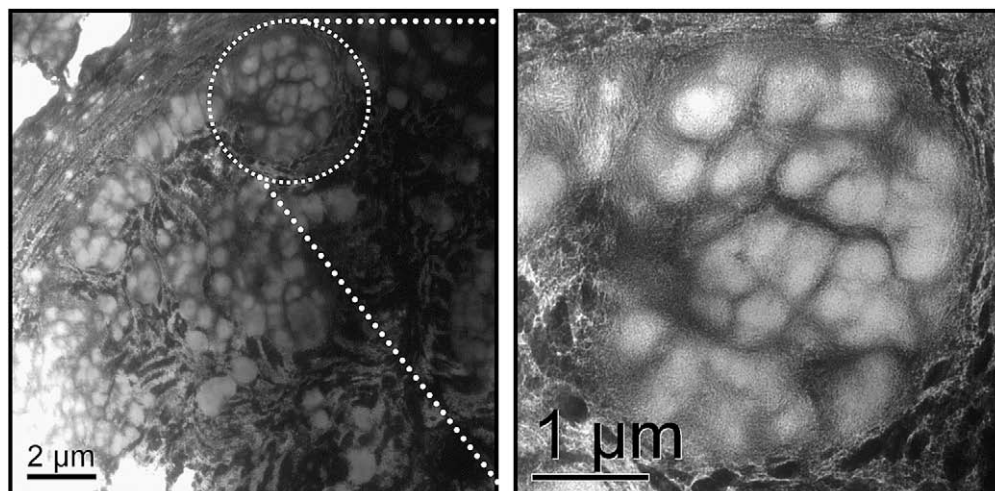
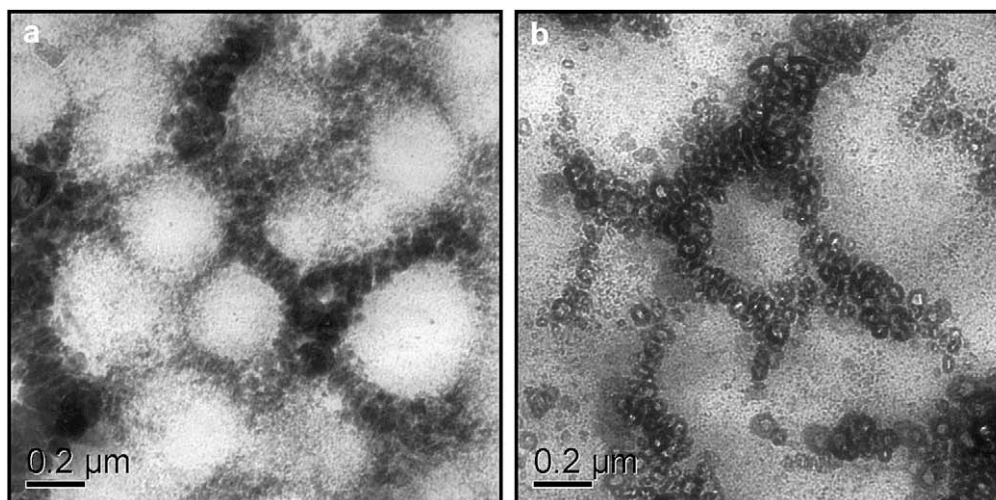


Fig. 4. TEM micrographs of a thin section of the hiPP particle after stained with  $\text{OsO}_4$  for 3 h.



**Fig. 5.** Close-up TEM micrographs of a thin section of the hiPP particle: (a) stained with OsO<sub>4</sub> for 3 h, (b) stained with RuO<sub>4</sub> for additional 0.5 h.

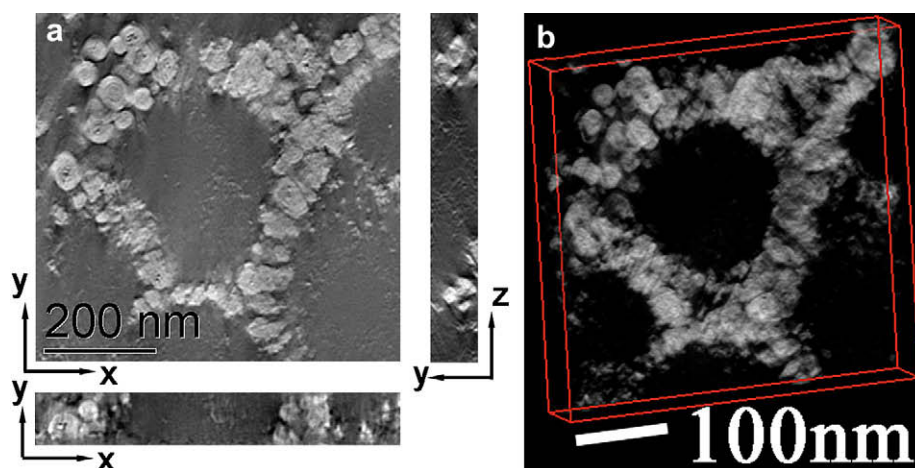
submicron-sized domains of 0.2–0.4 μm in diameter are full of sight (Fig. 4 left), which are clearly discerned as OsO<sub>4</sub>-unstainable PP domain (Fig. 4 right). The white PP domain include the crystalline PP and the amorphous PP. Dark domains appearing where the fissures, observed between PP domain, are large and become micropored.

Fig. 5(a) shows a close-up image of the above micrographs, stressing the micropores and fissures between the PP globules. Although somewhat blurry, it becomes distinguishable that the micropores between the PP globules are filled with dark, nano-sized microspheres. Obviously, it represents that the in situ-generated EP copolymers have been successfully stained by OsO<sub>4</sub>. To further distinguish these EP copolymers, another microtomed thin section was stained not only by OsO<sub>4</sub> for 3 h but also by RuO<sub>4</sub> for an additional 0.5 h. A close-up TEM image of this specimen is shown in Fig. 5(b), where the EP microspheres in between the PP globules clearly present themselves as nano-sized (ca. 30 nm in diameter) hollow droplets. These droplets are featured by a peripheric dark ring formed due to a preferential location of 1,7-octadiene at their outer surface causing more severe staining by RuO<sub>4</sub>.

To further confirm the above observed hiPP morphology, transmission electron microtomography (TEMT) images displaying

three-dimensional (3D) microstructure were recorded for the OsO<sub>4</sub> and RuO<sub>4</sub>-stained specimen. Fig. 6 shows the obtained 3D images of PP globules and EP microspheres in two different embodiments. It is obvious that a crack-free, quasi-spherical PP globule and the surrounding discrete but densely packed, nano-sized EP microspheres constitute the basic structure unit of the hiPP particle. Fig. 6 presents that the EP droplets connect with each other to form a network with a fractal structure. Wu has suggested that the toughness of rubber modified thermoplastics increased as inter-particle distance is reduced [20]. The inter-particle distance can be reduced either by increasing the rubber concentration or by decreasing the rubber particle size. The ductile-brittle transition will happen when the inter-particle distance between two nearest neighboring particles is at a critical value. In this case, the content of EPR is 18 wt%. The EP droplets connect with each other, and the inter-particle distance should have reached the critical value. The impact property of this system should be improved, and more detailed information will be discussed in a forthcoming paper.

Based on the above observations, it is manifest that the basic structure units comprising the whole hiPP particle are the sub-micron PP globule and nano-sized EP droplet. The formation of the PP globule is the results of the “hard” isotactic PP chains continuously crystallizing at the vicinity of a catalyst active site where they



**Fig. 6.** 3D reconstruction TEM micrographs of OsO<sub>4</sub> and RuO<sub>4</sub>-stained thin section of the hiPP particle: (a) an orthogonal cross-section of the 3D image, (b) 3D volume image.

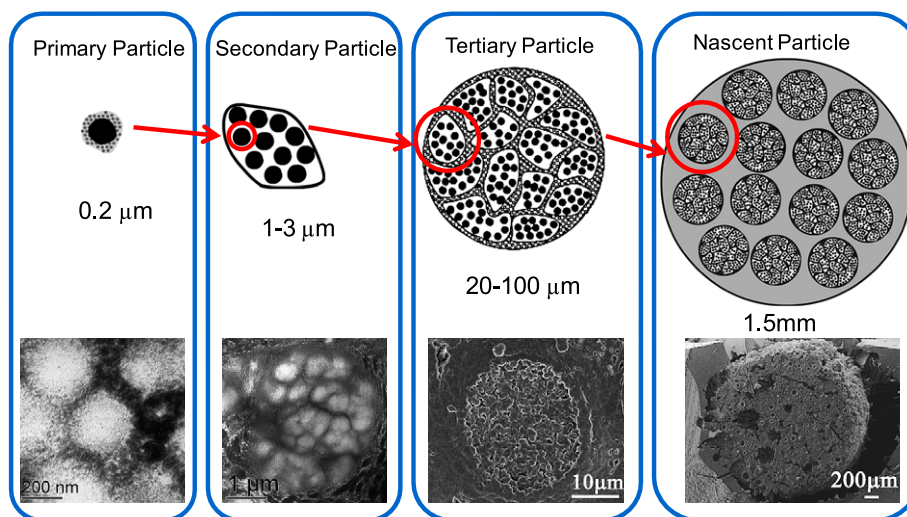


Fig. 7. Architecture of a nascent EP-P alloy particle with quaternary structures.

are released and pulled away from. The basic PP particle is composed of the crystalline PP and the amorphous PP. The multi-active sites on one primary catalyst particle (catalyst microparticle) render many PP domains, the individual expansion of which causes the formation of fissures. Diffusion of ethylene/propylene mixtures through these passages to the same active sites generates “soft”, uncrystallizable EP copolymer chains which, unlike “hard” PP chains, are unable to form their own domains. Instead, they are squeezed through the fissures between the preformed PP globule, forming small-sized droplets. Continuous E/P copolymerization produces a myriad of EP droplets, which flow into the micro- and macro-pores of the PP skeleton forming different-sized EPR droplets. This explains the continuous occurrence of E/P copolymerization, because the agglomeration of microspheric EP droplets is loose and will not block the micro- and macro-pores that are the monomers diffusion passages.

Taking the nano-sized EP droplets into account, a new quaternary structure model could be proposed to describe the structural hierarchy of the hiPP particles as well as to elucidate its course of formation (Fig. 7). During the first polymerization stage, propylene monomers are well dispersed and polymerized within the catalyst “reactor” that is composed of multiple levels of  $\text{MgCl}_2/\text{TiCl}_4$  agglomerates. The primary catalyst particles (catalyst microparticle) are responsible for the formation of the embryo primary PP globule (crystalline PP and amorphous PP,  $d = 200 \text{ nm}$ ) due to the in situ crystallization of PP chains at the vicinity of the active sites. In the second polymerization stage, ethylene and propylene monomers are believed to copolymerize on the same primary catalyst particle, which is tightly encompassed by several primary PP particles with fissures in between. Therefore, the formed EP copolymers are squeezed through fissures and become small-sized droplets. Continuous E/P copolymerization produces a myriad of EP droplets (Fig. 5), which flow into the micro- and macro-pores of the PP skeleton, forming different-sized EPR domains. Consequently, a nascent hiPP particle ( $d = 1.5 \text{ mm}$ ) consists of many tertiary particles (subglobule) of  $d = 20\text{--}100 \mu\text{m}$ , which are composed of smaller-sized secondary particles ( $d = 1\text{--}3 \mu\text{m}$ ). And the secondary particles are made of primary PP particles with a diameter of ca.  $200 \text{ nm}$  and nano-sized EP droplets.

This new hiPP structure model can help gain the essence of its high impact property. From the above results, the basic structure units, which constitute nascent hiPP particles are known to be the submicron PP globule and nano-sized EP droplet. The nano-sized

EP droplets can flow into most of the micro- and macro-pores in the preformed PP matrix, where it accumulates and eventually becomes EPR domains. This will ensure not only a full-length accommodation of EPR but also full measures of EPR dispersion and PP/EPR interfacial contact (percolation mechanism), which are accountable for the major causes of the high impact property of hiPP. Furthermore, as the micro- and macro-pores of the PP matrix are interconnected and form a network, the full-length distribution of EPR across the PP particle is apt to form a rubber network, which will also contribute to the high impact strength of hiPP.

#### 4. Conclusions

In conclusion, we have thrust into the very basic structural level of nascent hiPP particles and revealed that the basic structure units comprising a whole hiPP particle are the submicron PP globule and nano-sized EP droplet. EPR phase is formed by EP droplets agglomeration. Continuous formed EP droplets turn to fill, from inside out, the micro- and macro-pores inside preformed PP skeleton, forming different-sized EPR domains. The quaternary structures are for the first time proved to exist: the nascent EP-P particle ( $d = 1.5 \text{ mm}$ ), subglobule ( $d = 20\text{--}100 \mu\text{m}$ ), tertiary particle ( $d = 1\text{--}3 \mu\text{m}$ ), and primary particle ( $d = 200 \text{ nm}$ ). According to these findings, the control of first-staged propylene homopolymerization alongside a rational design of the catalyst architecture to optimize the dimensions and distributions of the micro- and macro-pores of the intermediate PP is crucial to obtain such a hiPP morphology that can warrant desired stiffness/toughness-balanced properties.

#### Acknowledgment

The financial supports from the National Natural Science Foundation of China (NSFC, Grant Nos. 20804054 and 20874104) and the National High-Tech R&D Program (863 Program) of China (2008AA030904, 2008AA030901) are gratefully acknowledged.

#### References

- [1] Galli P, Haylock JC. *Makromolekulare Chemie-Macromolecular Symposia* 1992;63:19.
- [2] Cecchin G, Morini G, Pelliconi A. *Macromolecular Symposia* 2001;173:195.
- [3] Galli P. *Journal of Macromolecular Science Part A* 1999;36:1561.
- [4] Fu ZS, Wang XF, Li N, Fan ZQ. *Journal of Polymer Materials* 2005;22:153.

- [5] Urdampilleta I, Gonzalez A, Iruin JJ, de la Cal JC, Asua JM. *Macromolecules* 2005;38:2795.
- [6] Chen Y, Chen W, Yang DC. *Polymer* 2006;47:6808.
- [7] Du J, Niu H, Dong JY, Dong X, Han CC. *Advanced Materials* 2008;20:2914.
- [8] Hutchinson RA, Chen CM, Ray WH. *Journal of Applied Polymer Science* 1992;44:1389.
- [9] Kakugo M, Miyatake T, Naito Y, Mizunuma K. *Macromolecules* 1988;21:314.
- [10] Kakugo M, Sadatoshi H, Sakai J, Yokoyama M. *Macromolecules* 1989;22:3172.
- [11] Kakugo M, Sadatoshi H, Yokoyama M. *Journal of Polymer Science Part C-Polymer Letters* 1986;24:171.
- [12] Noristi L, Marchetti E, Baruzzi G, Sgarzi P. *Journal of Polymer Science Part A-Polymer Chemistry* 1994;32:3047.
- [13] Nagel EJ, Kirillov VA, Ray WH. *Industrial & Engineering Chemistry Product Research and Development* 1980;19:372.
- [14] Schmeal WR, Street JR. *Aiche Journal* 1971;17:1188.
- [15] Schmeal WR, Street JR. *Journal of Polymer Science Part B-Polymer Physics* 1972;10:2173.
- [16] Cecchin G, Marchetti E, Baruzzi G. *Macromolecular Chemistry and Physics* 2001;202:1987.
- [17] McKenna TF, Soares JBP. *Chemical Engineering Science* 2001;56:3931.
- [18] Crowther RA, Derosier DJ, Klug A. *Proceedings of the Royal Society of London Series a-Mathematical and Physical Sciences* 1970;317:319.
- [19] Kakugo M, Sadatoshi H, Yokoyama M, Kojima K. *Macromolecules* 1989;22:547.
- [20] Wu S. *Polymer* 1985;26:1855.